Gas Processing Journal

Vol. 11, No. 2, 2023, pp. 11 - 22
http://gpj.ui.ac.ir

Research Paper

Simulation of Hydrogen Production Plant through Methane Steam Reforming Process in a Heat-Integrated Bayonet Tube Reactor

Alireza Palizvan [1], Amir Rahimi [1]*

[1] Department of Chemical Engineering, Faculty of Engineering, University of Isfahan, Isfahan, Iran

Received: 2024-07-26 Revised: 2025-01-17 Accepted: 2025-01-27

Abstract: An industrial hydrogen production plant is simulated through methane steam reforming process. A heat-integrated bayonet tube reactor, the key feature of which is separating the furnace and reactor tube constitute the main component of this process. The plant is a complex unit inoperation, where off-gas streams for burner fuel, flue gas are consumed for heating the feed and producing steam, next to having a complex structure of hydrogen production reactor. The plant simulation is run through the Aspen HYSYS software, and the hydrogen production reactor is modeled through Matlab software. The results indicate good agreement with plant data at different capacities. The Mean Absolute Relative Error (MARE) percentage for the outlet flue gas temperature, a crucial factor in predicting hydrogen production is 5. The MARE for steam production is below 3%. For the water-gas shift reactor, the MARE for outlet mole fractions and temperature is below 10%. These findings underscore the model's potential for predicting the performance of an industrial-scale hydrogen production unit accurately.

keywords: bayonet tube reformer; Steam methane reforming; Simulation of hydrogen production; convection reformer.

1. Introduction

In the chemical industry, hydrogen is a crucial reducing agent, consumed extensively in different processes. Its primary consumption is in refineries and methanol and ammonia production plants. The demand for hydrogen in the petroleum refining sector, due to consuming heavier crude oil types, which have higher sulfur and nitrogen content, next to stricter emissions regulations is on constant growth (Kar et al., 2023). Hydrogen has many applications in industries like metallurgy, electronics, pharmaceuticals, and food production (Bičáková & Straka, 2014). Given its growing significance in the energy sector, it is anticipated to be the fuel of the future, especially for fuel cells (Aminudin et al., 2023).

The biological fermentation, photocatalysis, fossil fuels, and water electrolysis are among the processes applied in hydrogen production (He et al., 2024). The Steam Methane Reforming (SMR) is known as the most feasible and well-established process for hydrogen generation (Aminudin et al., 2023). The SMR process is subject to the three primary reactions and the relevant Eqs. (1-3), which due to their high endothermic and heat transfer-limited features depend on efficient heat transfer.

$$CH_4 + H_2O \leftrightarrow CO + 3H_2 \qquad \Delta H_r|_{T=298\,K} = 206.1\ kJ/mol \tag{1}$$

$$CH_4 + 2H_2O \leftrightarrow CO_2 + 4H_2 \qquad \Delta H_r|_{T=298\,K} = 165\ kJ/mol \tag{2}$$

$$CO + H_2O \leftrightarrow CO_2 + H_2 \qquad \Delta H_r|_{T=298\,K} = -41.15\ kJ/mol \tag{3}$$

The focus of existing studies on SMR is on innovative techniques, like the reformers' heating electrically, applying microwaves for SMR plasma, and harnessing solar energy through molten salt to provide heat for the SMR process (Akande & Lee, 2022; Aminudin et al., 2023; De Falco et al., 2021; Giaconia et al., 2021). Running these process in the chemical industry is challenging, because most industrial reformers still rely on conventional burners for heat supply. The traditional burners, like top-fired, bottom-fired, side-fired, and terrace wall-fired reformers, are in common use (Amini et al., 2023). The drawbacks of these fired reformers are in their high volumes which require high fixed capital

* Corresponding Author.
Authors' Email Address: [1] A. Palizvan (palizvan96@gmail.com), [1] A. Rahimi (rahimi@eng.ui.ac.ir)

http://dx.doi.org/10.22108/GPJ.2025.142250.1138

costs, significant heat loss due to extensive surface areas, and high maintenance costs (M. M. Martín, 2016). Developing compact and efficient reformers is the major topic among the researchers with a focus on enhancing both design and operational parameters.

Convective reformers have been and are being proposed as an alternative to conventional radiant reformers. Hot gas from a combustion chamber is consumed in these reformers to supply the heat required for the reforming reactions, thereby avoiding direct contact and reducing the serious hot spots risk (Yu & Sosna, 2001). By eliminating the need for direct contact between the furnace and reactor tube, convective reformers offer a promising solution for improving efficiency and safety in this process reactions. This configuration is assessed by many researchers who have modeled reactors that analyze their own performance. Radiation effects are crucial in modeling the reactor accurately (Lim et al., 2024; Yu & Sosna, 2001). Amran et al. (Amran et al., 2017) applied a kinetic-based simulation of SMR and WGS reactions by applying a modified Langmuir-Hinshelwood-Hougen-Watson (LHHW) kinetic model in Aspen Plus, where the SMR reactor is assumed to be isothermal at 700°C feed inlet temperature, and sensitivity analysis is run to observe the operating conditions effect on reactor performance. Alrashed and Zahid (Alrashed & Zahid, 2021) simulated a Steam Methane Reforming (SMR) plant, by applying the Peng-Robinson thermodynamic model and assuming equilibrium reactions for the SMR process. In their study, a constant heat flux to the reactor wall was assumed, representing the heat flux supplied by the flue gas on the shell side; they performed optimization to determine the optimal operating conditions for the plant.

In another innovative configuration, double bayonet tubes are joined to convective reactors, which is of many advantages. In this configuration, the middle tube is full of catalyst, while the reformed gas exits through the central tube. The flue gas enters the outer tube to enhance heat recovery. This type of reactor is extensively assessed (Del Pópolo Grzona et al., 2024; Koo et al., 2023). Despite the promising findings, one significant limitation is the lack of validation against industrial data. The simulation of the entire plant to predict production rates is not adequately addressed yet. When the temperature exceeds 675◦C, the heat exchanger cost increases significantly (Ma et al., 2009). By applying superalloys only in high-temperature zones and conventional stainless steel in low-temperature zones, significant savings in equipment structural costs can be realized. This approach is integrated into industrial convective reformers, like the Haldor Topsoe Convection Reformer (HTCR), where a bayonet tube passes the flue gas through the outer cylinder (*Convection Reformer HTCR | Products | Equipment | Topsoe*, n.d.). The flue gas is produced in a furnace that burns natural gas and off-gas (returned flow from the Pressure Swing Adsorption (PSA) unit) with air. Steam is generated in a heat recovery vessel that captures energy from the process gas. Some heat-integrated exchangers consume flue gas for heating instead of hot oil. These factors contribute to the complexity of the simulation, emphasizing the need for a more reliable model.

To the best of the authors' knowledge, there exists no study on the simulation of a hydrogen production plant through a HTCR reactor. The objective here is to simulate hydrogen production through SMR by applying an HTCR reactor at different capacities. A one-dimensional heterogeneous model where the radiation effects are of concern in predicting the performance of the HTCR reactor, and the governing equations are solved in Matlab software. The other equipment in the plant are simulated in Aspen HYSYS software. This comprehensive simulation can contribute to the online prediction of plant performance at different capacities.

2. Process description

The process flow for the hydrogen production process is diagrammed in Fig. (1). The natural gas is mixed with the recycled hydrogen from the PSA unit and fed into the C-2601 A/B compressor, which increases pressure to 27.3 atm. The feed then passes through a heat exchanger, where it exchanges heat with the flue gas, raising temperature to 400°C. A temperature controller assures the feed stream's outlet temperature remains at 400 °C by recirculating part of the stream. The natural gas stream initially contains around 31 ppmv of sulfur compounds. The desulfurization process reduces these sulfur levels to below 0.05 ppmv, necessitating a hydrogen flow rate of 0.03 moles per second per mole of natural gas. The desulfurization section consists of the two: R-2601 and R-2602 reactors. The R-2601 reactor has: one hydrogenation and one sulfur absorption sections. The hydrogenation section with 1.65 m height is filled with a TK-250 catalyst (cobalt-molybdenum oxide). The main function of this section is to remove sulfur compounds and convert them into hydrogen sulfide through the following reaction:

$$COS + H_2 \longrightarrow CO + H_2S \quad (4)$$

$$R_1SR_2 + 2H_2 \longrightarrow R_1H + R_2H + H_2S \quad (5)$$

$$R_1SSR_2 + 3H_2 \longrightarrow R_1H + R_2H + 2H_2S \quad (6)$$

$$(CH)_4S + 4H_2 \longrightarrow C_4H_{10} + H_2S \quad (7)$$

$$RSH + H_2 \longrightarrow RH + H_2S \quad (8)$$

The second section of the R-2601 reactor with 2.8 m height, and R-2602 with 4.75 m bed height absorbs the produced hydrogen sulfide. These sections consume HTZ-3, which consists of activated zinc oxide as absorbent through the reaction expressed by reaction (9):

$$H_2S + ZnO \longrightarrow ZnS + H_2O \quad (9)$$

The desulfurized gas is mixed with superheated steam generated from E-2601 and is fed into the HTCR at 424°C. This reactor consists of 18 tubes inside one shell, where each consists of three concentric tubes, at a total length of 10 m. The schematic of the reactor and furnace X-2602 is shown in Fig. (2), where as observed the process gas enters the middle tube, from the top to initiate reforming reactions. The reformed gas exits the bottom of the reactor and enters the central tube, where it undergoes heat exchange with the middle tube. The gas exits from the top of the reactor for further processing. The flue gas leaving the furnace X-2602 enters the lower part of the reactor through the outer cylinder and after exchanging heat with middle tube, exits from the top of the reactor, allowing the required heat of reaction to be supplied from center and outer tube, thus, maintaining a configuration without the disadvantages associated with fired reformers. Next to uniform heat flow, the HTCR design has low volume and low capital costs compared to fired reformers. The flue gas is generated in a furnace separate from the reactor. The primary fuel for the furnace is the recycled off-gas from the Pressure Swing Adsorption (PSA) unit, supplemented by a natural gas stream and air. The flue gas exiting the (HTCR) passes through the E-2601, E-2605, and E-2606 heat exchangers to recover its heat before being released into the atmosphere at 255°C.

The syngas from HTCR enters the R-2603 reactor where CO converts into CO_2 and H_2 according to reaction (10).

$$CO + H_2O \leftrightarrow CO_2 + H_2 \quad (10)$$

The reactor is loaded with the SK-201-2 catalyst, consisting of copper and chromium on an iron support. At the beginning of operation with a new catalyst, the reactor inlet temperature is maintained at 340 °C, regulated by a controller integrated into the E-2602 heat exchanger, to control the process gas flow. As the catalyst is gradually deactivated over time, the inlet temperature can be increased gradually to assure that the reactor outlet temperature does not exceed 470 °C. The process gas exits reactor R-2603 at 399°C and flows into the tubes within vessel V-2601, designed to generate saturated steam. In unit 2600, three pieces of equipment are involved to generating the necessary steam: Vessel V-2601, where process gases enter the tube section and exit at 250°C. A portion of the water from vessel V-2601 is directed to heat exchanger E-2602. After exchanging heat with the process gas, this water generates some of the required steam and then returns to vessel V-2601. Another portion of the water from vessel V-2601 is directed to heat exchanger E-2606. After exchanging heat with the flue gas, this water generates additional required steam and then returns to vessel V-2601. The steam generated, after exchanging heat with the flue gas in heat exchanger E-2601 reaches 450°C, and is combined with the feed and then enters the HTCR reactor. The process gas stream then enters heat exchanger E-2604 A/B, where it is cooled to 163°C by the feed water to the V-2601, and enters the tubes of V-2604, a deaerator responsible for removing gases and dissolved solids from the incoming water. The demineralized water (DM water) enters the deaerator, where some of it evaporates, and the remaining water at 108°C is pumped by P-2601 A/B. A pressure controller on the process gas stream entering V-2604 regulates the vessel's pressure by bypassing the gas stream.

After cooling to 149 °C, the process gas enters the air cooler FA-2602, to become colder by air. In the warm season, the gas cools down to 60 °C, and in the cold season up to 25 °C. The process gas first enters the heat exchanger E-2608, where it is cooled to 33 °C by cooling water, next enters V-2602, which acts as a phase separator to remove water from the gas stream and assure that the PSA unit receives water-free gas and then process enters section X-2601. This section consists of four beds producing hydrogen a 99.9% purity. The unit's recovery rate (the hydrogen output flow to the hydrogen input flow rate ratio) is approximately 0.6:0.8. Changes in unit capacity do not affect recovery or product purity; (even if the input flow rate is reduced to 30% of the maximum design flow rate), the recovery remains constant. However, recovery decreases at capacities below 30%. The unit has two output streams: 1) the product stream, containing hydrogen, and 2) the off-gas stream, primarily composed of hydrogen and carbon dioxide. The off-gas stream is sent to furnace X-2602 for combustion. Some of the hydrogen is recycled to be combined with natural gas at the beginning of the unit.

The unit's capacity is defined as the hydrogen production flow rate to the hydrogen flow rate ratio at 100% capacity (2727 Nm^3/h)

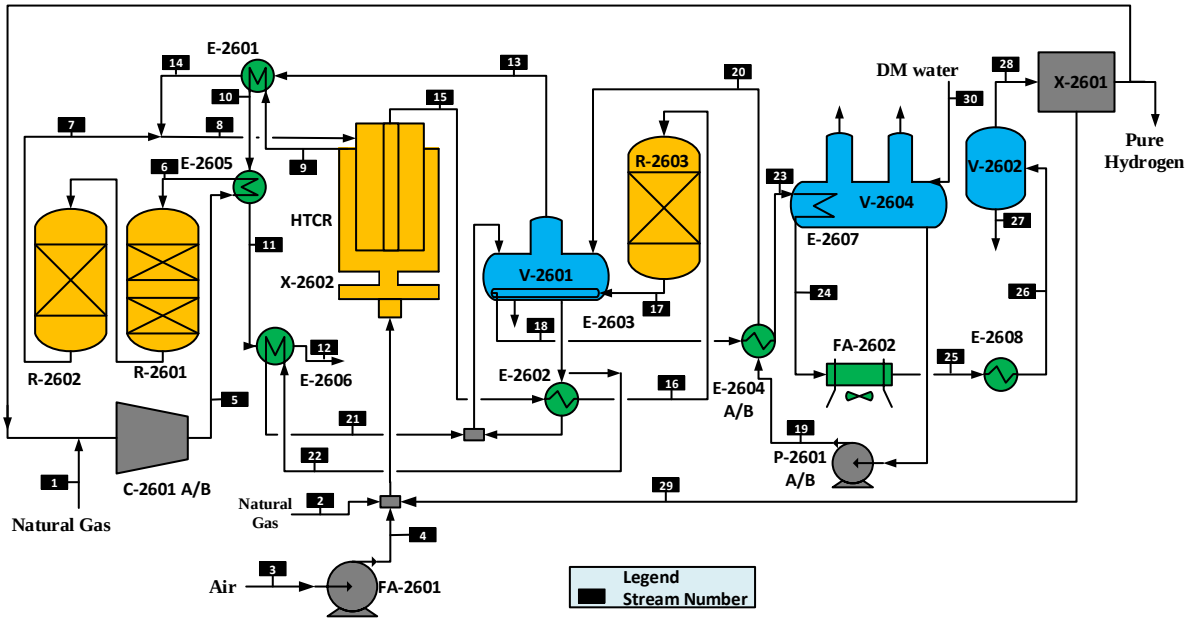

Fig. 1. Process flow diagram of hydrogen production with HTCR reactor (Topsoe, 2002)

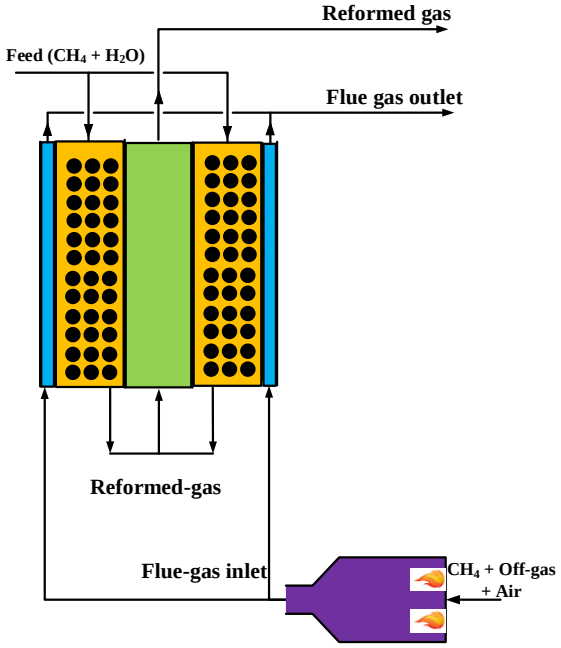

Fig. 2. Schematic of HTCR and X-2602

3. Plant simulation procedure

Due to the presence of water in the system, the PRSV thermodynamic model is applied for the simulation in Aspen HYSYS V10. To simulate C-2601 A/B, FA-2601 (the blower for supplying air to X-2602), and P-2601 A/B, the outlet pressure and efficiency are involved. The polytropic efficiency for both the compressor and blower is given by the vendor as 0.7. Because the pump's efficiency has a negligible effect on the outlet water temperature, the adiabatic efficiency of the pump is unknown but assumed 0.75.

To simulate heat exchangers E-2601 through E-2608 and FA-2602, their dimensions are given as the input data into Aspen Exchanger Design and Rating V10, and fed into Aspen HYSYS. With the specified input conditions, the software calculates the output temperature and pressure. Controllers are installed on heat exchangers E-2601, E-2602, E-2605, and E-2607 to adjust the incoming gas stream flow rate. The simulation process is as follows:

- For heat exchangers E-2601, E-2602, and E-2605, the input flow rate is adjusted through Tee and Adjust to assure that the desired output conditions are met
- Heat exchanger E-2607, a tube inside vessel V-2604, receives process gas that transfers heat to the water, causing partial evaporation. The input flow rate must be regulated to maintain constant pressure in the vessel. Because the water evaporation rate at different capacities is not known, the input gas flow rate is adjusted through the Adjust and Tee to reach to a steam generation rate of 100 kg/h. This value is derived from the 100% production capacity. The water level and pressure in V-2604 remain constant at different unit capacities

The flow rates of the water streams entering heat exchangers E-2602 and E-2606 are unknown, and no flow meters are installed on the pipelines. Given that the water level in vessel V-2601 remains constant, it can be reasonably assumed that the flow rates entering the heat exchangers are constant and equal to the values reported in the equipment datasheets. This assumption is supported by the reported error margins discussed in the results section.

In V-2601, the two blowdown streams regulate water quality: 1) the continuous, assumed to be 32 kg/h at all capacities, and 2) the intermittent (not considered due to its negligible amount). Heat exchanger E-2608 operates with a cooling water stream, at constant water flow rate at all capacities.

Due to the negligible sulfur content in the feed and the lack of detailed information on sulfur compounds compositions, reactors R-2601 and R-2602 are not simulated. It is assumed that the hydrogen in the recycle stream is not consumed. Reactor R-2603 is simulated through an equilibrium reactor model, with the equilibrium constant supplied by the software. Because in this context this assumption is not universally valid, it should be validated vs. the experimental data. According to the vendor's documentation (Topsoe, 2002), the reactor operates under near-equilibrium conditions, holding this assumption reasonable.

For simulation the PSA unit (X-2601), a material separator is applied. Due to the absence of adsorption isotherms' data and the complexity of dynamic simulation, a separator is applied to isolate all hydrogen. The hydrogen is split into product and off-gas streams through the Tee and efficiency adjustments. The unit recovery is calculated through Eq. (4).

$$\text{Hydrogen recovery in simulation} = 1 - \frac{\text{Hydrogen flow rate in off-gas (unit data)}}{\text{Hydrogen flow rate to PSA unit inlet (unit data)}} \quad (4)$$

The furnace X-2602 is simulated as a conversion reactor where the following reactions are of concern:

$$C_4H_{10} + 6.5O_2 \longrightarrow 4CO_2 + 5H_2O \quad (11)$$
$$1.5O_2 + CH_4 \longrightarrow CO + 2H_2O \quad (4)$$
$$C_3H_8 + 5O_2 \longrightarrow 3CO_2 + 4H_2O \quad (5)$$
$$0.5O_2 + CO \longrightarrow CO_2 \quad (6)$$
$$H_2 + 0.5O_2 \longrightarrow H_2O \quad (7)$$
$$C_2H_6 + 3.5O_2 \longrightarrow 2CO_2 + 3H_2O \quad (8)$$
$$C_4H_{10}(\text{isobutane}) + 6.5O_2 \longrightarrow 4CO_2 + 5H_2O \quad (9)$$

The HTCR reactor is modeled in Matlab R2022a through a one-dimensional, heterogeneous approach that incorporates radiative heat transfer effects (Palizvan & Rahimi, 2024). The kinetics of the reaction for Ni supported on an alumina catalyst are provided by (Xu & Froment, 1989). The integration between Matlab and Aspen HYSYS allows for a comprehensive and accurate simulation of the process.

4. Results and discussion

The simulation results are compared with the plant data. To determine the simulation error for each piece of equipment, the following methodology is adopted: the input specifications for each piece of equipment (excluding the flue gas flow rate, which was derived from the simulation) are fed to the software. The simulation outputs for each piece of equipment are compared with the corresponding industrial data. This approach assures that the error for each piece of equipment does not effect others. The analyses from different sections are based on a dry basis (excluding water vapor). The steam flow rate is calculated through an overall mass balance. The unit's capacity is determined based on the flow rate of pure hydrogen exiting the PSA unit, where 2727 Nm^3/h flow rate corresponds to 100% capacity, and other capacities are specified relative to this capacity. The 54% unit capacity is selected as the base case where the Absolute Relative Error (ARE) is reported. To assure the

accuracy of the simulation at different capacities, the Mean Absolute Relative Error (MARE) is reported for the unit operating at 98%, 62%, 62%, and 57% capacities. Comparison of outlet temperatures between simulation and plant data (T^{s}_{out} and T^{P}_{out}, respectively) for heat exchangers E-2601 to E-2608, FA-2602, compressor C-2601 A/B, and blower FA-2601 are tabulated in Table 1. To determine the error for the pump, the outlet temperature is required; though, this parameter is not measured in the unit. Given that the temperature change in water due to pressure is negligible, the error associated with this equipment is disregarded. The composition and temperature of the inlet air into FA-2601 are unknown, and this fact increases the simulation error. The specifications assumed for the air simulation are tabulated in Table 2. Due to the lack of data on the input and output water flows for heat exchanger E-2602, and the controlled outlet gas temperature, it is not possible to report the error for this equipment. The process gas temperature in the E-2602 outlet is not measured, thus the simulation error for this equipment is not reported; consequently, the inlet temperature to FA-2602 is obtained from the software. The inlet air temperature to the heat exchanger is selected approximately. The process gas, after passing through E-2608, enters a two-phase separator. The gas outlet temperature of E-2608 is not measured; while, the gas outlet temperature from vessel V-2602 is available. This temperature is applied to calculate the error for E-2608. As discussed in the simulation section, the water flow rate entering E-2602 and E-2606 is considered constant at all capacities. The steam production rate and output from V-2601 are known in the unit. Therefore, the simulation error for this equipment is a proper criterion for validating the made assumption. It is observed that the error is less than 3%. The simulation results for the outlet compositions of furnace X-2602 are shown in Fig. 3(a). No CO gas is observed at the furnace outlet, and NOx gases are not measured. MARE for H2O is relatively high due to the uncertainty of the inlet composition, while for other components, it remains below 10%. The simulation results for the outlet compositions of reactor R-2603 are bar-charted in Fig. 3(b), the average of all errors is less than 10%, thus, acceptable. Consequently, the initial assumption that the reactor operates under near-equilibrium conditions is validated for the simulated capacities, though, it may not hold for other operating conditions. For the PSA section, the feed gas to this section is sampled. The outlet water flow rate from V-2602 and the composition of the gas exiting can be determined through a mass balance. The simulation results and comparison with industrial data for the outlet of V-2602 (PSA unit inlet) are tabulated in Table 1. The analysis and composition of the off-gas stream, next to the flow rates, are specified. The simulation error for the PSA section, are tabulated in Table 1, where the hydrogen production rate has an average error of 13.6%, which is acceptable. The higher error in the nitrogen composition can be attributed to its low numerical value and the associated mass balance error. The results for the outlet composition of the HTCR reactor are presented in Fig. 3(c), where, the average error across all parameters is less than 10%. The mole fraction of hydrogen exhibits the lowest error among the mole fractions, with an average relative error of 3.6%. The results for pressure drop and gas flow rate are tabulated in Table 1, where the error in the pressure drop within the reactor is higher than expected due to the omission of minor losses in the calculations. The comparison between the simulation results and plant data for the outlet temperatures of the reactors is illustrated in Fig. 3(d), where, the MARE for predicting the outlet temperature of reactor X-2602, given the simulation assumptions, is within an acceptable range of 5%. Accurate prediction of the flue gas temperature exiting the furnace is critical for estimating hydrogen production, as the majority of the reaction heat is supplied by the flue gas. For the HTCR, the model's error in predicting the outlet temperature of the central tube about 5 % is higher than that for other tubes. In contrast, the MARE for the outlet gas temperature of reactor R-2603 is significantly lower, at 1.8%. A summary of the main stream specifications shown in Fig. (1) is provided in Table A.1 of Appendix A.

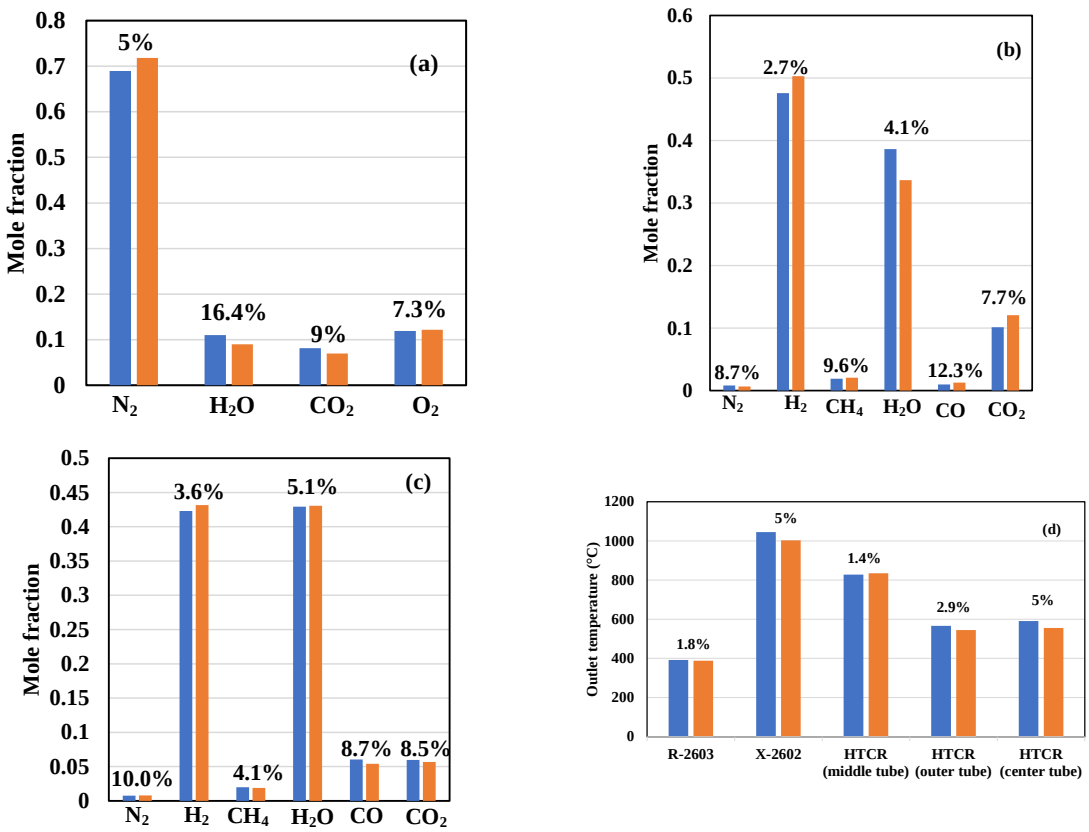

Fig. 3. Comparison of simulation results (blue bars) and plant data (orange bars) for (a) outlet compositions of X-2602, (b) outlet compositions of R-2603, (c) outlet compositions of HTCR, and (d) outlet temperatures of R-2603, X-2602, and HTCR with the MARE over each bar

Table 1. Comparison of simulation results and plant data

C-2601 A/B, FA-2601, E-2601-E-2608, FA-2602				
Equipment	**T^{s}_{out} (°C)**	**T^{P}_{out} (°C)**	**ARE (%)**	**MARE (%)**
C-2601 A/B	80	91	13.0	11.4
FA-2601	76	106	28.3	27.1
E-2601	464	437	6.2	5.8
E-2603	242	234	3.4	3.7
E-2604 Gas phase	161	164	2.1	1.8
Liquid phase	210	210	0.2	2.6
E-2605	405	388	4.5	5.7
E-2606	240	243	1.0	1.1
E-2608	25	26	3.3	1.4
FA-2602	13	23	44.7	43.2
V-2601				
Parameter	**Simulation data**	**Plant data**	**ARE (%)**	**MARE (%)**
Steam flow rate (Nm^3/h)	2299	2329	1.7	2.8
R-2603				

Parameter at outlet	Simulation data	Plant data	ARE (%)	MARE (%)
Flow rate (Nm^3/h)	3536	3594	1.6	1.6

X-2602

Parameter at outlet	Simulation data	Plant data	ARE (%)	MARE (%)
Flow rate (Nm^3/h)	7527	7352	2.4	5.4

V-2602

Parameter at outlet	Simulation data	Plant data	ARE (%)	MARE (%)
Water flow rate (Nm^3/h)	1206	1250	3.5	3.1
Mole fractions:				
N_2	0.0100	0.0100	0.01	0.01
H_2	0.7568	0.7568	0.01	0.01
CH_4	0.0310	0.0310	0.01	0.01
H_2O	0.0017	0.0015	10.98	10.62
CO	0.0190	0.0190	0.01	0.01
CO_2	0.1816	0.1817	0.06	0.06
Gas flow rate (Nm^3/h)	2388	2292	4.2	2.3

PSA

Parameter at outlet	Simulation data	Plant data	ARE (%)	MARE (%)
Pure hydrogen flow rate (Nm^3/h)	1288	1472	12.5	13.6
Off-gas mole fractions:				
N_2	0.0228	0.0149	52.5	149.9
H_2	0.4450	0.4464	0.3	7.8
CH_4	0.0706	0.0807	12.5	9.1
H_2O	0.0035	0.0035	0.3	7.8
CO	0.0433	0.0448	3.4	11.3
CO_2	0.4148	0.4096	1.3	5.6
Off-gas flow rate (Nm^3/h)	1004	1001	0.3	9.7

HTCR

Parameter at outlet	Simulation data	Plant data	ARE (%)	MARE (%)
Gas flow rate in middle tube (Nm^3/h)	2.4006	2.4344	1.4	2.0
Outlet gas pressure in middle tube (atm)	22.48	22.30	0.8	1.3
Pressure drop (atm)	0.08	0.26	69.3	71.5

Table 2. Air specifications for simulation

Parameter	Value
Temperature (°C)	12 for the autumn and winter seasons 30 for the spring and summer seasons
Mole fractions:	
O_2	0.2177
CO_2	0.0003
N_2	0.7720
H_2O	0.01

5. Conclusion

The simulation of a hydrogen production plant through MSR and applying a heat-integrated reactor is run here. A one-dimensional heterogeneous model incorporating radiation effects is applied for reactor simulations, while Aspen HYSYS is applied for other types of equipment. The validation of results is made at different plant capacities. For the heat exchangers, the MARE is below 6% except for the air cooler due to a lack of exact information about air specifications in different season. The prediction of the flue gas temperature as an important factor is 5%. The MARE of steam produced in V-2601 is below 3%. For the WGS reactor, the MARE of outlet mole fractions and temperature is below 10%.

These findings indicate the flexibility of simulation for the prediction of hydrogen production and can be applied for further studies like the exergy and economic analysis.

Appendix A. Stream Specifications

Table A.1 presents the detailed specifications of the main streams depicted in Fig. 1, including flow rates, compositions, temperatures, pressures, and other relevant parameters.

Table A.1. Specifications of the main streams depicted in Fig. 1

Stream number	1	2	3	4	5	6	7	8
Vapour fraction	1.00	1.00	1.00	1.00	1.00	1.00	1.00	1.00
Temperature (°C)	9.5	7.7	12	76	80	400	358	545
Pressure (atm)	12.56	1.07	0.82	1.35	25.01	24.99	24.77	0.91
Molar flow rate (Nm^3/h)	515	77	6693	6693	529	529	529	7527
Mass flow rate (kg/h)	400	60	8595	8595	401	401	401	9644
Mole fractions:								
Oxygen	0.0000	0.0000	0.2177	0.2177	0.0000	0.0000	0.0000	0.1219
Hydrogen	0.0000	0.0000	0.0000	0.0000	0.0270	0.0270	0.0270	0.0000
Nitrogen	0.0510	0.0510	0.7720	0.7720	0.0496	0.0496	0.0496	0.7178
Carbon monoxide	0.0000	0.0000	0.0000	0.0000	0.0000	0.0000	0.0000	0.0000
Carbon dioxide	0.0030	0.0030	0.0003	0.0003	0.0029	0.0029	0.0029	0.0701
Methane	0.9100	0.9100	0.0000	0.0000	0.8855	0.8855	0.8855	0.0000
Water	0.0000	0.0000	0.0100	0.0100	0.0000	0.0000	0.0000	0.0902
Ethane	0.0270	0.0270	0.0000	0.0000	0.0263	0.0263	0.0263	0.0000
Propane	0.0060	0.0060	0.0000	0.0000	0.0058	0.0058	0.0058	0.0000
Butane	0.0020	0.0020	0.0000	0.0000	0.0019	0.0019	0.0019	0.0000
Isobutane	0.0010	0.0010	0.0000	0.0000	0.0010	0.0010	0.0010	0.0000

Stream number	10	11	12	13	14	15	16	17
Vapour fraction	1.00	1.00	1.00	1.00	1.00	1.00	1.00	1.00
Temperature (°C)	464	405	240	229	449	555	343	392
Pressure (atm)	0.86	0.78	0.84	26.95	26.93	22.30	22.27	22.25
Molar flow rate (Nm^3/h)	7527	7527	7527	2339	2339	3536	3536	3536
Mass flow rate (kg/h)	9644	9644	9644	1880	1880	2078	2078	2078
Mole fractions:								
Oxygen	0.1219	0.1219	0.1219	0.0000	0.0000	0.0000	0.0000	0.0000
Hydrogen	0.0000	0.0000	0.0000	0.0000	0.0000	0.4315	0.4315	0.4758
Nitrogen	0.7178	0.7178	0.7178	0.0000	0.0000	0.0080	0.0080	0.0080
Carbon monoxide	0.0000	0.0000	0.0000	0.0000	0.0000	0.0541	0.0541	0.0098
Carbon dioxide	0.0701	0.0701	0.0701	0.0000	0.0000	0.0569	0.0569	0.1012
Methane	0.0000	0.0000	0.0000	0.0000	0.0000	0.0188	0.0188	0.0188
Water	0.0902	0.0902	0.0902	1.0000	1.0000	0.4307	0.4307	0.3864
Ethane	0.0000	0.0000	0.0000	0.0000	0.0000	0.0000	0.0000	0.0000
Propane	0.0000	0.0000	0.0000	0.0000	0.0000	0.0000	0.0000	0.0000
Butane	0.0000	0.0000	0.0000	0.0000	0.0000	0.0000	0.0000	0.0000
Isobutane	0.0000	0.0000	0.0000	0.0000	0.0000	0.0000	0.0000	0.0000

Stream number	18	19	20	21	22	23	24	25
Vapour fraction	1.00	0.00	0.00	0.07	0.00	0.94	0.84	0.66
Temperature (°C)	242	111	210	229	229	161	148	13
Pressure (atm)	22.22	32.75	32.70	26.92	26.95	22.18	22.15	22.01
Molar flow rate (Nm^3/h)	3595	2139	2157	14367	14367	3595	3595	3595
Mass flow rate (kg/h)	2127	1720	1733	11547	11547	2127	2127	2127
Mole fractions:								
Oxygen	0.0000	0.0000	0.0000	0.0000	0.0000	0.0000	0.0000	0.0000
Hydrogen	0.5028	0.0000	0.0000	0.0000	0.0000	0.5028	0.5028	0.5028
Nitrogen	0.0066	0.0000	0.0000	0.0000	0.0000	0.0066	0.0066	0.0066
Carbon monoxide	0.0126	0.0000	0.0000	0.0000	0.0000	0.0126	0.0126	0.0126
Carbon dioxide	0.1207	0.0000	0.0000	0.0000	0.0000	0.1207	0.1207	0.1207
Methane	0.0206	0.0000	0.0000	0.0000	0.0000	0.0206	0.0206	0.0206
Water	0.3367	1.0000	1.0000	1.0000	1.0000	0.3367	0.3367	0.3367
Ethane	0.0000	0.0000	0.0000	0.0000	0.0000	0.0000	0.0000	0.0000
Propane	0.0000	0.0000	0.0000	0.0000	0.0000	0.0000	0.0000	0.0000
Butane	0.0000	0.0000	0.0000	0.0000	0.0000	0.0000	0.0000	0.0000
Isobutane	0.0000	0.0000	0.0000	0.0000	0.0000	0.0000	0.0000	0.0000

Stream number	26	27	28	29	30
Vapour fraction	0.66	0.00	1.00	1.00	0.00
Temperature (°C)	25	26	26	26	20
Pressure (atm)	22.00	22.00	22.00	22.04	1.48
Molar flow rate (Nm^3/h)	3595	1206	2388	1004	2265
Mass flow rate (kg/h)	2127	970	1157	995	1821

Mole fractions:					
Oxygen	0.0000	0.0000	0.0000	0.0000	0.0000
Hydrogen	0.5028	0.0000	0.7568	0.4450	0.0000
Nitrogen	0.0066	0.0000	0.0100	0.0228	0.0000
Carbon monoxide	0.0126	0.0000	0.0190	0.0433	0.0000
Carbon dioxide	0.1207	0.0002	0.1816	0.4148	0.0000
Methane	0.0206	0.0000	0.0310	0.0706	0.0000
Water	0.3367	0.9998	0.0017	0.0035	1.0000
Ethane	0.0000	0.0000	0.0000	0.0000	0.0000
Propane	0.0000	0.0000	0.0000	0.0000	0.0000
Butane	0.0000	0.0000	0.0000	0.0000	0.0000
Isobutane	0.0000	0.0000	0.0000	0.0000	0.0000

References

Akande, O., & Lee, B. (2022). Plasma steam methane reforming (PSMR) using a microwave torch for commercial-scale distributed hydrogen production. *International Journal of Hydrogen Energy*, *47*(5), 2874–2884. https://doi.org/https://doi.org/10.1016/j.ijhydene.2021.10.258

Alrashed, F., & Zahid, U. (2021). Comparative analysis of conventional steam methane reforming and PdAu membrane reactor for the hydrogen production. *Computers & Chemical Engineering*, *154*, 107497. https://doi.org/https://doi.org/10.1016/j.compchemeng.2021.107497

Amini, A., Anaraki Haji Bagheri, A., Sedaghat, M. H., & Rahimpour, M. R. (2023). CFD simulation of an industrial steam methane reformer: Effect of burner fuel distribution on hydrogen production. *Fuel*, *352*, 129008. https://doi.org/https://doi.org/10.1016/j.fuel.2023.129008

Aminudin, M. A., Kamarudin, S. K., Lim, B. H., Majilan, E. H., Masdar, M. S., & Shaari, N. (2023). An overview: Current progress on hydrogen fuel cell vehicles. *International Journal of Hydrogen Energy*, *48*(11), 4371–4388. https://doi.org/https://doi.org/10.1016/j.ijhydene.2022.10.156

Amran, U. I., Ahmad, A., & Othman, M. R. (2017). Kinetic based simulation of methane steam reforming and water gas shift for hydrogen production using aspen plus. *Chemical Engineering Transactions*, *56*, 1681–1686. https://doi.org/10.3303/CET1756281

Bičáková, O., & Straka, P. (2014). *The resources and methods of hydrogen production*. *7*, 175–188.

Convection reformer HTCR | Products | Equipment | Topsoe. (n.d.). Retrieved March 26, 2024, from https://www.topsoe.com/our-resources/knowledge/our-products/equipment/convection-reformer-htcr

De Falco, M., Santoro, G., Capocelli, M., Caputo, G., & Giaconia, A. (2021). Hydrogen production by solar steam methane reforming with molten salts as energy carriers: Experimental and modelling analysis. *International Journal of Hydrogen Energy*, *46*(18), 10682–10696. https://doi.org/https://doi.org/10.1016/j.ijhydene.2020.12.172

Del Pópolo Grzona, M. V., Pedernera, M. N., & López, E. (2024). Two-zone convective reformer for the decentralized production of H2/syngas from biomethane. *International Journal of Hydrogen Energy*, *59*, 845–855. https://doi.org/https://doi.org/10.1016/j.ijhydene.2024.01.343

Giaconia, A., Iaquaniello, G., Morico, B., Salladini, A., & Palo, E. (2021). Techno-economic assessment of solar steam reforming of methane in a membrane reactor using molten salts as heat transfer fluid. *International Journal of Hydrogen Energy*, *46*(71), 35172–35188. https://doi.org/https://doi.org/10.1016/j.ijhydene.2021.08.096

He, W., Liu, T., Ming, W., Li, Z., Du, J., Li, X., Guo, X., & Sun, P. (2024). Progress in prediction of remaining useful life of hydrogen fuel cells based on deep learning. *Renewable and Sustainable Energy Reviews*, *192*, 114193. https://doi.org/https://doi.org/10.1016/j.rser.2023.114193

Kar, S. K., Sinha, A. S. K., Harichandan, S., Bansal, R., & Balathanigaimani, M. S. (2023). Hydrogen economy in India: A status review. *Wiley Interdisciplinary Reviews: Energy and Environment*, *12*(1), e459.

Koo, Y., Kang, S., Ra, H., Yoon, S., & Ryu, C. (2023). Numerical Evaluation of Heat Transfer and Conversion Efficiency by Tube Design and Flow Configuration for a Compact Steam-Methane Reformer. In *Energies* (Vol.

16, Issue 22). https://doi.org/10.3390/en16227475

Lim, T.-W., Hwang, D.-H., & Choi, Y.-S. (2024). Design and optimization of a steam methane reformer for ship-based hydrogen production on LNG-fueled ship. *Applied Thermal Engineering*, *243*, 122588. https://doi.org/https://doi.org/10.1016/j.applthermaleng.2024.122588

Ma, T., Xie, G. N., & Wang, Q. W. (2009). *Thermal Design of a High Temperature Bayonet Tube Heat Exchanger With Inner and Outer Fins* (pp. 291–296). https://doi.org/10.1115/GT2009-60283

Martín, M. M. (2016). *Chapter 5 - Syngas* (M. M. B. T.-I. C. P. A. Martín & Design (Eds.); pp. 199–297). Elsevier. https://doi.org/https://doi.org/10.1016/B978-0-08-101093-8.00005-7

Palizvan, A., & Rahimi, A. (2024). *Multi-Scale Modeling of Hydrogen Production Via Steam Reforming in a Heat-Integrated Bayonet Tube Rector*. https://doi.org/10.2139/SSRN.4823014

Topsoe. (2002). *Operating Manual for Hydrogen Production Plant, Iran Chemical Industries Investment Company (ICIIC). Internal document provided by ICIIC.*

Xu, J., & Froment, G. F. (1989). Methane steam reforming, methanation and water-gas shift: I. Intrinsic kinetics. *AIChE Journal*, *35*(1), 88–96. https://doi.org/10.1002/aic.690350109

Yu, Y. H., & Sosna, M. H. (2001). Modeling for Industrial Heat Exchanger Type Steam Reformer. *Korean Journal of Chemical Engineering*, *18*(1), 127–132. https://doi.org/10.1007/BF02707209